The International Archives of the Photogrammetry, Remote Sensing and Spatial Information Sciences, Volume XLVIII-1/W3-2023
2nd GEOBENCH Workshop on Evaluation and BENCHmarking of Sensors, Systems and GEOspatial Data
in Photogrammetry and Remote Sensing, 23–24 October 2023, Krakow, Poland

# EVALUATING A NADIR AND AN OBLIQUE CAMERA FOR 3D INFRASTRUCTURE (CITY) MODEL GENERATION

K. G. Nikolakopoulos [1] *, A. Kyriou [1]

[1] GIS & Remote Sensing Laboratory, University of Patras, Department of Geology, 26504, Patras, knikolakop@upatras.gr, a.kyriou@upnet.gr)

**Commission II**

**KEY WORDS:** UAV, Nadir, Oblique, accuracy, RMSE.

**ABSTRACT:**

The analysis of Earth's surface is strongly associated with the creation of three dimensional representations. In light of this, researchers involved in any realm of research as, geological, hydrological, ecological planning, city modelling, civil infrastructure monitoring, disaster management and emergency response, require 3D information of high fidelity and accuracy. For many decades, aerial photos or satellite data and photogrammetry provided the necessary information. In recent years, high-resolution imagery acquired by Unmanned Aerial Vehicles (UAV) has become a cost-efficient and quite accurate solution. In this framework, an infrastructure-monitoring project, named called "PROION", focuses among others on the generation of very fine and highly accurate 3D infrastructure (city) model. The specific study evaluates a high-resolution nadir camera and an oblique camera for the creation of a 3D representation of the Patras University Campus. During the project, two identical flights over a part of the campus were conducted. The flights were performed with a vertical take-off and landing (Vtol) fixed wind UAV equipped with PPK receiver on-board. Based on the conducted flights, many data sets have been evaluated regarding the accuracy and fidelity. It was proved that both nadir and oblique cameras produced very accurate 3D representations of the University campus buildings. The RMSE error of the nadir imagery is almost two times higher than the respective error of the oblique imagery reaching 30cm.

## 1. INTRODUCTION

For more than three decades, aerial photos or high-resolution satellite data and photogrammetry provided the necessary 3D information for diverse studies such as city modelling, civil infrastructure monitoring, disaster management and emergency response. Moreover, a study comparing nadir and oblique imagery for the 3D representation of two historical buildings in Bordeaux, France, has been presented (Pepe et al., 2022). Imagery was acquired by a Leica airborne sensor and processed using Structure from Motion (SfM) photogrammetry. In recent years, aerial images acquired by an Unmanned Aerial Vehicle (UAV) and point clouds derived from terrestrial or airborne laser scanners have become a commonplace for 3D reconstruction of photorealistic building models due to the cost-effectiveness and convenience. Oblique photogrammetry based on aerial images acquired by UAVs has proved to be quite effective and precise for the creation of high-quality 3D building models (Haala and Kada 2010; Remondino et al. 2011; Colomina et al. 2014; Nex and Remondino 2014; Pajares, 2015).

Harwin et al. (2015) investigated the joint use of nadir and oblique imagery for a coastal cliff representation in south-eastern Tasmania, Australia. They carried out twenty-eight different scenarios, using ground control point's of diverse accuracy (centimetre to millimetre levels) and examining the gcp's allocation inside the study area. In addition, the suitability of nadir and oblique imagery and SfM photogrammetry has been evaluated for the reconstruction of high-resolution topography and geomorphic features of quarries (Rossi et al., 2017). In particular, a hexacopter equipped with a Canon EOS 550D DSLR camera was used to acquire the images and the processing was performed with two of the most known commercial software (i.e. Pix4d and Agisoft Photoscan). Added to this, reference data acquired with a total station (Leica TCR 1200+ series) were used the validation of the results. A similar study over a very steep site in Saudi Arabia (i.e. slopes varying from 0 to 90 degrees) was performed by Tu et al., 2021. Four sets of images including diverse combinations of nadir, oblique and façade imagery i.e. a) only nadir imagery, b) nadir and oblique imagery, c) nadir and façade imagery and d) nadir, oblique, and façade imagery, were used to reconstruct a topographically complex natural surface. The results were validated with reference data collected with a Terrestrial Laser Scanner (TLS).

TLS data has been also utilized as reference in another similar study (Aicardi et al., 2016.) In that study, diverse combination of oblique images obtained by UAV were tested for the 3D reconstruction of a historical building, i.e. the S. Maria Chapel, a part of the Novalesa Abbey (Italy). In a similar study, the acquisition and use of oblique images acquired by a low cost UAV to reconstruct historical architectures was evaluated (Lingua et al., 2017). TLS and GNSS data were used to evaluate the results.

The relation that may exist between the acquisition geometry of UAV campaigns (nadir, oblique) and the topographic characteristics of an investigated area, in the framework of landslide mapping and monitoring activities, has been examined in two recent studies (Kyriou et al. 2021; Nikolakopoulos et al. 2022). The specific studies investigated the role of the image acquisition geometry in different areas in Greece with diverse morphological characteristics. It was proved that the acquisition of UAV oblique and nadir imagery as well as the synergistic processing increased the overall centimetre accuracy.

At the same time, there are also studies assessing the effectiveness of UAV nadir and oblique imagery for 3D building representation. In such a study (Vacca et al., 2017) nadir and oblique imagery was processed with two software (Pix4d and Agisoft Photoscan) and the results of a single

building reconstruction were validated with reference data obtained from TLS.
In light of creating high accuracy 3D models, UAV and TLS products were used within PROION project (Nikolakopoulos et al. 2022). The specific project proposes an infrastructure monitoring methodology based on remote sensing and in situ measurements. Two crucial infrastructure located in the Western Greece, i.e. a) the building of Geology Department in the University of Patras and b) a fresh water dam called Asteri dam, are surveyed using data from SAR interferometry, GNSS and micro-accelerometers sensors. In this context, there is a need for very fine and highly accurate 3D infrastructure (city) model to serve as a base map. The specific study evaluates the spatial resolution and accuracy of 3D data derived from two cameras mounted on a Vtol fixed wind UAV.

## 2. CAMERAS, SURVEYS, PROCESSING

### 2.1 Cameras

Both cameras are adjustable payloads on a Trinity F90+ UAV. The nadir camera is a Sony RX1 RII model with 42.4 MP (7952 × 5304) resolution. The sensor is a full frame format, extracting high quality and high-resolution imagery (1.29cm at 100m above ground level).
The oblique camera is a five-lens RGB camera, named Oblique D2M. Each of the five cameras has 26 MP (6252 x 4168) resolution resulting to a total of 130 MP. The sensor is APS-C format that is able to generate high quality and high-resolution imagery (1.5cm at 100m above ground level).

### 2.2 Surveys

Two flight campaigns (around thirty minutes' flight time each), over a specific area of the Patras University campus were performed. A Trinity F90+ vertical take-off and landing fixed wind UAV was used. The same photogrammetric grid with 70% overlap along the track and 70% overlap across the track was repeated. The UAV is equipped with a PPK receiver and therefore the images were georeferenced. The nadir survey collected 434 photos, while the oblique survey produced 2165 images (433 images x 5 cameras). The total volume of the first survey was 14.5 GB, whereas the respective volume for the second one was 11.4 GB (Table 1).

### 2.3 Processing

Agisoft Metashape software was used for the processing of the two data sets. The exact same parameters (Ultra high accuracy) were used during the different processing steps. The processing was carried out on a desktop with a ninth generation (I9) Intel processor (Intel(R) Core(TM) i9-10850K CPU @ 3.60GHz), 128 GB of RAM, SDD disk and a NVIDIA GeForce RTX 3080 graphic card. The whole processing in both cases took more than one week.

### 2.4 Reference data

Several ground control points were measured using a double frequency GNSS receiver (Leica GS08 RTK) on the ground level and on the buildings of the campus. The Leica GS08 Plus GNSS receiver was used without a dedicated base station, but with differential position corrections from the Greek Hellenic Positioning System (HEPOS) – through GSM network- and Real-Time Kinematic (RTK). The receiver is capable of GPS (L1, L2 and L2C frequencies), GLONASS (L1 and L2 frequencies) and SBAS (WAAS, GAGAN, MSAS and EGNOS systems). The accuracy specifications for this receiver are 10 mm + 1 ppm horizontally and 20mm+1 ppm vertically. During the execution of GCPs measurements, the horizontal RMSE was ranging between the values 0.9 cm and 1.3 cm, whereas the vertical RMSE varied between 1.4 cm and 1.9 cm. Reference data from classical topographic survey used in the past for the construction of the buildings were also utilized.

## 3. RESULTS

The processing generated three new data sets that were compared and analysed in more details. Specifically, the products are categorized as:

- 3D point clouds
- Digital Surface Model of the campus
- Orthophoto of the campus

The results are discussed in detail in the following paragraphs.

### 3.1 3D point clouds

The 3D point cloud emerged from the oblique camera acquisitions consisted of more than 4.7 million points (Figure 1). This cloud was compared with the respective one derived from the nadir camera acquisitions, comprising of 2.7 million points. The statistics of the two point clouds are presented in Table 1. It is remarkable that despite the fact that the two flight campaigns followed the same photogrammetric grid the oblique cloud covered a larger area (1.21 $km^2$) than the nadir-viewing one (0.817$km^2$). This outcome is related to the existence of the 5 cameras on the Oblique D2M, which look at different directions and are able to produce 3D points outside of the grid area. Moreover, it is notable that nadir imagery extracted a point cloud with higher point density (i.e. 0.32 points/cm) compared to the oblique imagery that generated a point cloud with lower point density (0.24 points/cm). Since the flight altitude remained the same for the execution of both surveys, this outcome is probably associated with the higher resolution of the nadir camera i.e. 42MP. The Leica Cyclone Suite was used for the comparison of the 3D models; however, the procedure was affected by the volume of the two point clouds making the comparison a time consuming and demanding task. In this framework further research is planned.

| | Oblique | Nadir |
|---|---|---|
| No of images | 2165 | 434 |
| Raw data Volume | 11.4 GB | 14.5 GB |
| No of points | 4.7M | 2.7M |
| Spatial resolution | 2.04 cm | 1.77 cm |
| Point density | 0.24 points/cm | 0.32 points/cm |
| Coverage area | 1.21 $km^2$ | 0.817 $km^2$ |

**Table 1**. Cloud statistics.

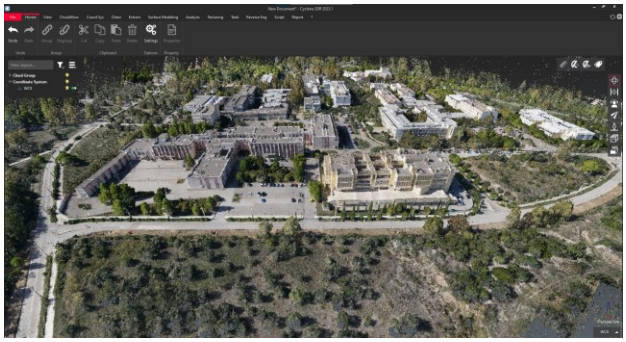

**Figure 1**. 3D point cloud from the oblique camera.

### 3.2 Orthophotos

Orthophotos were emerged from the processing of the two different data sets in Agisoft Photoscan software. The two products were compared in ArcMap. The accuracy, the spatial resolution and the fidelity of the orthoimages were evaluated in GIS environment using reference data from classical topographic surveys. Oblique orthophoto has a spatial resolution of 2.04cm while the respective resolution of the nadir orthophoto is 1.77cm (Table 1). The difference is spatial resolution is obvious between the structural features of the buildings. Specifically, a characteristic example of such comparison is depicted in Figure 2, in which the red rectangle indicates the selected building. Figures 2b and 2c display the nadir and oblique orthophoto of the specific building.

Despite the slightly higher spatial resolution of the nadir orthophoto (i..e. 1.77 cm instead of 2.04 cm of the oblique orthophoto), the oblique-viewing products represent better the structural features located on the roof of the building. As it can be observed in Figure 2c, a sunroof created by concrete is established on the roof of the building. Such construction cannot be detected on the nadir orthophoto. At the same time, the patio existing inside the building can be easily and thoroughly identified in Figure 2c, but it looks blurred in Figure 2b. In general, the oblique orthophoto represents in more detail structural elements that present even small differences in elevation.

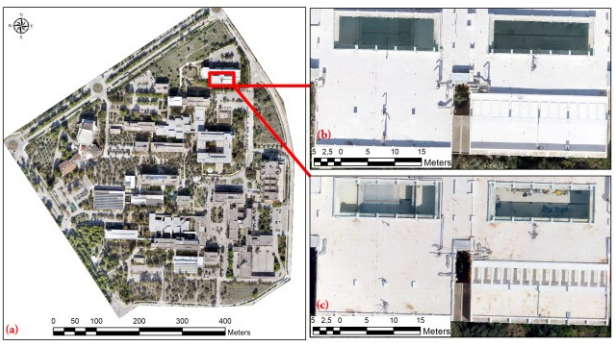


**Figure 2**. **(a)** Oblique orthophoto of the campus. **(b)** The roof of a building as depicted in the nadir orthophoto. **(c)** The same roof as depicted in the oblique orthophoto.

### 3.3 Digital Surface Models

Two Digital Surface Models were derived from either the nadir-viewing camera (Figure 3) or the oblique one (Figure 4). The statistics of the two DSMs are presented in Table 2. Generally speaking, the two DSMs exibited similar statistical values. In particular, the mean elevation value of the oblique DSM is 39.897, while the respective value for the nadir DSM is 39.70m. Furthermore, the variation between the standard deviation values between the generated DSMs was calculated at 0.153m. On the contrary, the maximum and the minimum values display remarkable differences.

To precisely identify and analyse the DSM variations, we subtracted the nadir DSM form the oblique one in a GIS environment. The outcome displaying the differences is depicted in Figure 5. In particular, the mean elevation difference was computed at 0.198m, while the standard deviation value was calculated at 1.164m. As it can be observed in Figure 5 the higher elevation differences marked in magenta (positive values) or yellow (negative values) colour are detected mainly outside of the buildings. It is worth mentioning that the extent of the buildings, illustrated with red rectangular, was derived from topographic survey. The magenta and yellow spots, observed outside of the red rectangles, correspond to vegetation canopy differences or to vehicles that were moved during the flights.

| | Oblique | Nadir |
|---|---|---|
| Minimum | -45.151 | -58.37 |
| Maximum | 134.82 | 126.59 |
| Mean | 39.897 | 39.70 |
| Median | 53.972 | 54.039 |
| St. Deviation | 30.143 | 29.990 |

**Table 2**. DSMs statistical values (in m).

The accuracy of the Digital Surface Models regarding building's height was investigated using GNNS measurements. Figure 3 presents the DSM created from the nadir images while the respective DSM from the oblique imagery is presented in Figure 4. The two DSMs present an almost identical representation of the campus. Buildings, vegetation canopy, pavements and vehicles can be easily recognized in both DSMs. It is remarkable that even the low pavements can be identified and recognized.

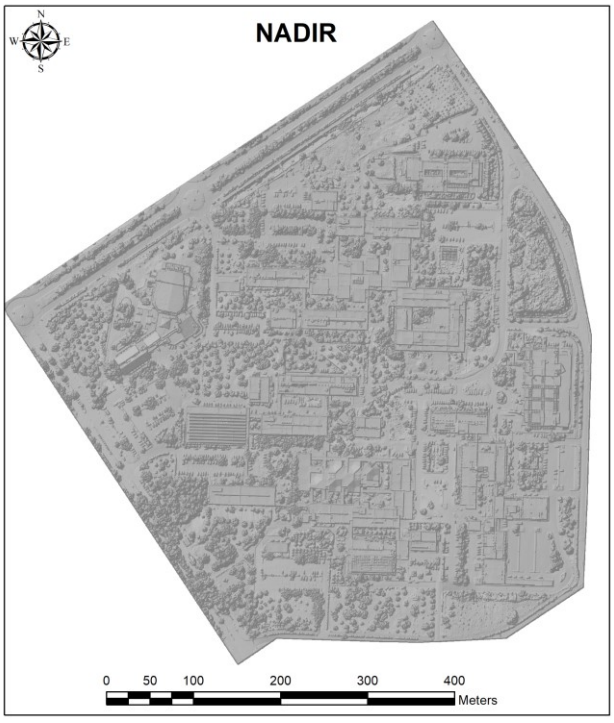


**Figure 3**. DSM created from the nadir images

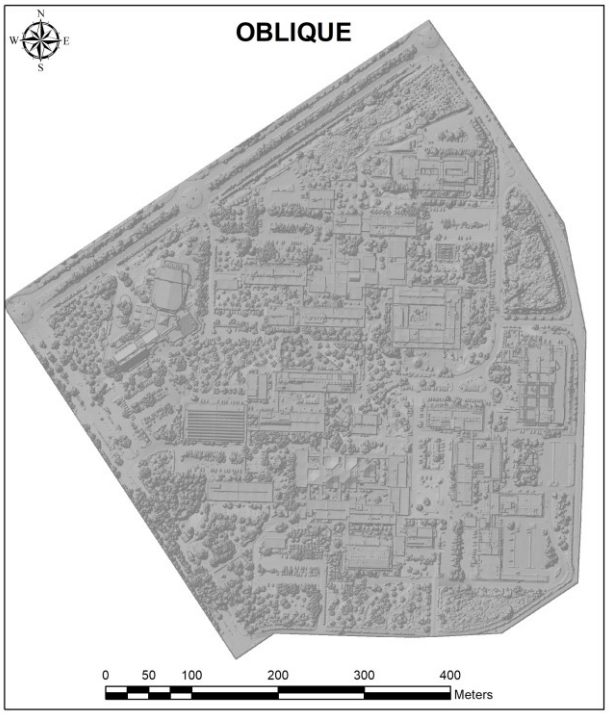


**Figure 4**. DSM created from the oblique images

To accurately assess the elevation differences the polygons of the buildings were used to crop the DSMs. Two new DSMs containing only the building elevation data were created and compared (Figure 6 and figure 7).

**Figure 5**. **(a)** DSM difference. The nadir DSM was subtracted from the oblique DSM **(b)** The roof of the building as depicted in the nadir DSM. **(c)** The same roof as depicted in the oblique DSM.

As it can be observed in Figure 6a there is a characteristic linear element with magenta colour that corresponds to an elevation difference between 1 and 2m. The specific linear feature corresponds to a sun power panel (Figure 6b). The panel can be easily recognized in the oblique DSM (Figure 6d), while it is not detectable in the nadir DSM (Figure 6c).

**Figure 6**. **(a)** A characteristic spot with DSM difference higher than 5m. **(b)** The height difference corresponds to a sun power panel as it can be observed in the oblique orthophoto **(c)** The same roof as depicted in the nadir DSM. **(d)** The same roof as depicted in the oblique DSM

A similar case demonstrating the lower accuracy of the nadir DSM is presented in Figure 7. As it can be noted inside the red rectangle (Figure 7a) there are linear features with magenta or yellow colour. The magenta color is correlated with positive elevation difference values while the yellow colour corresponds to negative difference values. In figure 7b it is obvious that there are roofs with tiles on the top of the building. These tiled roofs are separated and there is a gap between them. Mechanical equipment such as air conditioning units can be recognized in this gap. The elevation difference provoked by the mechanical equipment is detected on the DSM from the oblique imagery (Figure 7d). In the DSM from the nadir images (Figure 7c) these elevation differences cannot be easily identified. In general, it is proved that features with small elevation difference such as small walls, sunroofs or equipment cannot be detected on the nadir DSM.

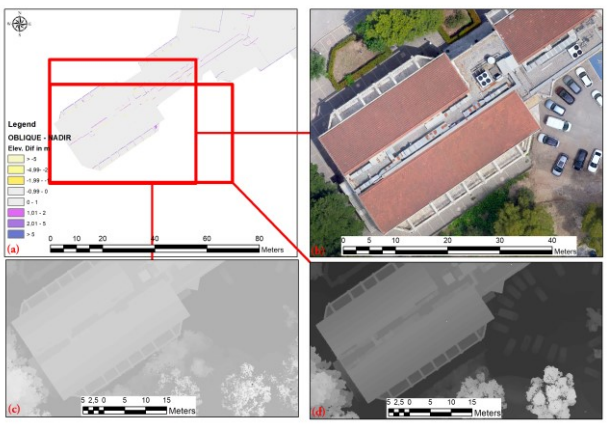

**Figure 7. (a)** A characteristic spot with DSM difference higher than 5m**. (b)** The height difference corresponds to the gap between the two roofs **(c)** The same roof as depicted in the nadir DSM. **(d)** The same roof as depicted in the oblique DSM

### 3.3.1 Digital Surface Models accuracy assessment

Ground control points (gcps) were collected with RTK GNSS sensor on the ground and at different levels within the building

boundaries. The distribution of gcps is presented in Figure 8, where 34 measured points located inside and outside of a building in diverse heights are marked as red dots. The elevation values of these points were extracted using the DSMs in an ArcMap environment. In addition, the elevation difference between GNSS measurement and DSM height were calculated and the outcomes are presented in Table 3. As it can be observed the oblique DSM is more accurate than the nadir DSM. The lowest difference is 9cm, while the highest is 20cm. The oblique DSM presents an average elevation difference from the GNSS measurements of 14.6cm while the respective difference for the nadir DSM is almost double at 29.6cm. The Root Mean Square Error for the oblique DSM was estimated at 15cm while the RMSE for the nadir DSM is at 30cm.

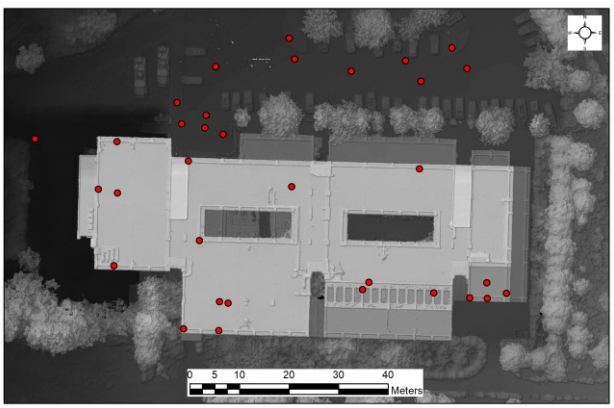


**Figure 8.** One of the building that were used for the elevation accuracy control of the two DSMs. Red bullets correspond to the GNSS measurements.

| GCP's No | GNSS - nadir | GNSS - Oblique |
|---|---|---|
| GPS00034 | 0,3184 | 0,1391 |
| GPS00033 | 0,3045 | 0,1436 |
| GPS00032 | 0,3144 | 0,1245 |
| GPS00031 | 0,3175 | 0,1448 |
| GPS00030 | 0,3065 | 0,1461 |
| GPS00029 | 0,2953 | 0,1497 |
| GPS00029 | 0,2804 | 0,1529 |
| GPS00028 | 0,3579 | 0,1569 |
| GPS00027 | 0,5150 | 0,3512 |
| GPS00026 | 0,3355 | 0,1805 |
| GPS00025 | 0,3560 | 0,1826 |
| GPS00024 | 0,3346 | 0,1574 |
| GPS00023 | 0,3624 | 0,1961 |
| GPS00022 | 0,3295 | 0,1989 |
| GPS00021 | 0,3466 | 0,1789 |
| GPS00020 | 0,3371 | 0,1961 |
| GPS00019 | 0,3243 | 0,1773 |
| GPS00018 | 0,2700 | 0,1172 |
| GPS00017 | 0,2177 | 0,1070 |
| GPS00016 | 0,2132 | 0,1188 |
| GPS00015 | 0,2564 | 0,1139 |
| GPS00014 | 0,2646 | 0,1093 |
| GPS00013 | 0,2791 | 0,1287 |
| GPS0012 | 0,2618 | 0,1243 |
| GPS0011 | 0,2608 | 0,1233 |
| GPS0010 | 0,2985 | 0,1383 |
| GPS0009 | 0,2716 | 0,1388 |
| GPS0008 | 0,2648 | 0,1236 |
| GPS0007 | 0,2831 | 0,1131 |
| GPS0006 | 0,2451 | 0,1030 |
| GPS0005 | 0,2650 | 0,1187 |
| GPS0004 | 0,2672 | 0,1208 |
| GPS0003 | 0,2267 | 0,1100 |
| GPS0002 | 0,2509 | 0,1175 |
| GPS0001 | 0,2489 | 0,1214 |
| **Average** | **0,2966** | **0,1464** |

**Table 3**. Elevation differences between RTK GNSS measurements and DSMs values (in m).

## 4. DISCUSSION

The comparison the generated products proved that the oblique imagery can provide better results in 3D representation of buildings within the campus of the University of Patras. The specific outcome is in accordance with previous studies. Aicardi et al. (2016) mentioned that the use of oblique images acquired from UAV is an effective tool to survey Cultural Heritage objects, which are characterized by limited accessibility, need for detail and rapidity of the acquisition phase, and often reduced budgets. In addition, Yu et al., (2021) proved that the synergistic collection of oblique and façade imagery can facilitate the more conservative nadir acquisitions, improving significantly the geometric accuracy of point cloud data reconstruction by approximately 35% when assessed against terrestrial laser scanning data of near-vertical rock walls. Rossi et al., (2017) stated that the execution of exclusively nadir viewing is not an appropriate approach for surveying sub-vertical walls while the combined use of nadir and oblique imagery is able to strengthen the consistency of the reconstructed surfaces. Similar to our study, Vacca et al., (2017) proved that oblique UAV flights increase the achievable accuracy in terms of the number of points in a point cloud, and in the generated 3D models. Even with the absence of ground control points systematic errors in the DSM creation can be significantly decreased when oblique imagery is used as mentioned by James and Robson (2014).

## 5. CONCLUSIONS AND FUTURE WORK

Products derived from a nadir and an oblique camera mounted on the same Vtol UAV, following the same photogrammetric grid, were examined in order to create 3D infrastructures (city) models in the frame of PROION Project.

It is proved that the oblique camera produce 3D representation of higher accuracy in comparison to the nadir. The RMSE error of the oblique camera is only 15cm while the respective RMSE of the nadir camera raises to 30cm.
Especially, to create 3D representation of buildings the oblique camera is more suitable as it can distinguish small objects on the roof of the buildings such as the external air-condition units, sun roofs etc.
This research will continue in two directions:

1. More detailed comparison of the 3D point clouds and comparison to respective data from TLS
2. Detection and analysis of all the outliers in order to better understand the pros and cons of each camera.

## ACKNOWLEDGEMENTS

This research has been co-financed by the European Regional Development Fund of the European Union and Greek national funds through the Operational Program Competitiveness, Entrepreneurship and Innovation, under the call RESEARCH – CREATE – INNOVATE (project code: T2EΔK-02396 Multiparametric monitoring platform with micro-sensors of eNceladus hellenIc supersite)».

## REFERENCES

Aicardi, I., Chiabrando F., Grasso, N., Lingua, A. M., Noardo, F., Spanò, A., 2016. UAV photogrammetry with oblique images: first analysis on data acquisition and processing. The International Archives of the Photogrammetry, Remote Sensing and Spatial Information Sciences, Volume XLI-B1, XXIII ISPRS Congress, 12–19 July 2016, Prague, Czech Republic doi:10.5194/isprsarchives-XLI-B1-835-2016.

Colomina, I., Molina, P., 2014. Unmanned aerial systems for photogrammetry and remote sensing: A review. ISPRS J. Photogramm. Remote Sens., 92, 79–97.

Haala,N., Kada,M., 2010. An update on automatic 3D building reconstruction. ISPRS J. Photogramm. Remote Sens., 65, 570–580.

Harwin, S., Lucieer, A., Osborn, J., 2015. The Impact of the Calibration Method on the Accuracy of Point Clouds Derived Using Unmanned Aerial Vehicle Multi-View Stereopsis. Remote Sens. 2015, 7, 11933-11953. https://doi.org/10.3390/rs70911933

James, M.R., Robson, S., 2014. Mitigating systematic error in topographic models derived from UAV and ground-based image networks. Earth Surface Processes and Landforms, 39(10), 1413–1420. doi:10.1002/esp.v39.10

Kyriou, A., Nikolakopoulos, K., Koukouvelas, I., 2021. How Image Acquisition Geometry of UAV Campaigns Affects the Derived Products and Their Accuracy in Areas with Complex Geomorphology. ISPRS Int. J. Geo-Inf., 10, 408. https://doi.org/10.3390/ijgi10060408

Lingua A., Noardo F., Spanò A., Sanna S., Matrone F., 2017. 3D model generation using oblique images acquired by UAV, The International Archives of the Photogrammetry, Remote Sensing and Spatial Information Sciences, Volume XLII-4/W2, FOSS4G-Europe 2017 – Academic Track, 18–22 July 2017, Marne La Vallée, France https://doi.org/10.5194/isprs-archives-XLII-4-W2-107-2017

Massimiliano P., Fregonese L, Crocetto N., 2022. Use of SfM-MVS approach to nadir and oblique images generated through aerial cameras to build 2.5D map and 3D models in urban areas, Geocarto International, 37:(1), 120-141, https://doi.org/10.1080/10106049.2019.1700558

Nex, F., Remondino, F., 2014. UAV for 3D mapping applications: A review. Appl. Geomat., 6, 1–15.

Nikolakopoulos K. G., Kyriou A., Sokos E., Bousias S., Strepelias E., Groumpos P., Mpelogianni V., Roumelioti Z., Serpetsidaki A., Paliatsas D., Stephanopoulos P., Ganas A., Charalampoulou V., and Athanasopoulos T., 2022. Multiparametric microsensor monitoring platform of the Enceladus Hellenic supersite: the PROION project. Proc. SPIE 12268, Earth Resources and Environmental Remote Sensing/GIS Applications XIII, 122680K https://doi.org/10.1117/12.2638830

Nikolakopoulos, K.G., Kyriou, A., Koukouvelas, I.K., 2022. Developing a Guideline of Unmanned Aerial Vehicle's Acquisition Geometry for Landslide Mapping and Monitoring. Appl. Sci., 12, 4598. https://doi.org/10.3390/app12094598.

Pajares, G., 2015. Overview and current status of remote sensing applications based on unmanned aerial vehicles (UAVs). Photogramm. Eng. Remote Sens., 81, 281–330.

Remondino, F., Barazzetti, L., Nex, F., Scaioni, M., Sarazzi, D., 2011. UAV photogrammetry for mapping and 3d modeling–current status and future perspectives Int. Arch. Photogramm. Remote Sens. Spat. Inf. Sci., 38, C22.

Rossi P., Mancini F., Dubbini M., Mazzone F., Capra A., 2017. Combining nadir and oblique UAV imagery to reconstruct quarry topography: methodology and feasibility analysis, European Journal of Remote Sensing, 50:1, 211-221, DOI: 10.1080/22797254.2017.1313097

Tu Y.H., et al., 2021. Combining Nadir, Oblique, and Façade Imagery Enhances Reconstruction of Rock Formations Using Unmanned Aerial Vehicles, IEEE Transactions on Geoscience and Remote Sensing, vol. 59, no. 12, pp. 9987-9999, Dec. 2021, doi: 10.1109/TGRS.2020.3047435.

Vacca, G., Dessì, A., Sacco, A., 2017. The Use of Nadir and Oblique UAV Images for Building Knowledge. ISPRS Int. J. Geo-Inf. 2017, 6, 393. https://doi.org/10.3390/ijgi6120393